atmosphere

MDPI

Article

Sensitivity of Source Apportionment of Ambient $PM_{2.5}$-Bound Elements to Input Concentration Data

Tianchu Zhang [1], Yushan Su [2,*], Jerzy Debosz [2], Michael Noble [2], Anthony Munoz [2] and Xiaohong Xu [1,*]

[1] Department of Civil and Environmental Engineering, University of Windsor, Windsor, ON N9B 3P4, Canada; zhang14g@uwindsor.ca
[2] Ontario Ministry of the Environment, Conservation and Parks, Toronto, ON M9P 3V6, Canada; jerzy.debosz@ontario.ca (J.D.); michael.noble@ontario.ca (M.N.); tony.munoz@ontario.ca (A.M.)
* Correspondence: yushan.su@ontario.ca (Y.S.); xxu@uwindsor.ca (X.X.)

Abstract: This study investigated the sensitivity of the positive matrix factorization (PMF) model using concentrations of $PM_{2.5}$-bound elements in Windsor, Ontario, Canada. Five scenarios were devised to assess impacts of input data on source identification, source contributions, and model performance. The study found that the model outcomes and performance were not sensitive to data below method detection limits (MDLs) being replaced with 1/2 MDLs, nor whether brown carbons (BrCs) data were excluded. By analyzing two episodic events individually, unique factors of fireworks and mineral dust were identified for each of the two episodes. Moreover, PMF model performance was improved greatly for event markers of the episodes and elements with less variability in concentration when compared with the base case scenario. Excluding the two episodes from the entire dataset had little impact on factor identification and source contributions but improved the model performance for three out of twelve elements unique to the two episodes. Overall, the PMF model outcomes and performance were sensitive to percentages of concentrations below MDLs and element concentrations with large variability due to high concentrations observed in episodes. Our findings are useful for dealing with data below MDLs and episodic events in conducting future PMF source apportionment of $PM_{2.5}$-bound elements.

Keywords: $PM_{2.5}$; trace elements; source apportionment; sensitivity; MDL (method detection limits); episodic events

Citation: Zhang, T.; Su, Y.; Debosz, J.; Noble, M.; Munoz, A.; Xu, X. Sensitivity of Source Apportionment of Ambient $PM_{2.5}$-Bound Elements to Input Concentration Data. *Atmosphere* **2023**, *14*, 1269. https://doi.org/10.3390/atmos14081269

Academic Editor: Avelino Eduardo Saez

Received: 1 June 2023
Revised: 21 July 2023
Accepted: 7 August 2023
Published: 10 August 2023

1. Introduction

Fine particulate matter ($PM_{2.5}$) consists of particles that are 2.5 μm or less in diameter. $PM_{2.5}$ is emitted directly and formed by reactions of gaseous precursors in the air. $PM_{2.5}$ is a complex mixture of solid particles and liquid droplets [1,2]. Major components of $PM_{2.5}$ include organic compounds, dust, soot, and metals. Trace elements of $PM_{2.5}$ are found in natural environments (e.g., mineral dust) and are emitted from anthropogenic activities such as metal processing, coal burning, mining, and road traffic [3]. Exposure to ambient $PM_{2.5}$ is associated with a wide range of health outcomes, including premature mortality and respiratory and cardiovascular diseases [4]. $PM_{2.5}$ is one of the criteria air pollutants identified by Environment and Climate Change Canada (ECCC) [5] and by the United States Environmental Protection Agency (USEPA) [6]. Canadian Ambient Air Quality Standards (CAAQS) were developed for $PM_{2.5}$ based on the scientific evidence of health and environmental effects and are used as air quality objectives under the Canadian Environmental Protection Act to drive continuous improvement of air quality across Canada [7,8]. To communicate health risks associated with air pollution, $PM_{2.5}$ was also one of the three air pollutants that were included in Ontario's Air Quality Health Index (AQHI) when it was implemented in 2015 [9]. The 2020 annual mean value of $PM_{2.5}$ in Ontario was 6.2 $\mu g/m^3$, a 17% decrease compared to that in 2011, owing to effective emission controls which led to an 18% reduction in $PM_{2.5}$ emissions [10]. This annual concentration is below

the Ontario annual AAQC of 8.8 μg/m^3 but higher than annual average concentrations of 5 μg/m^3 recommended by the World Health Organization (WHO) [11]. The significant reductions in $PM_{2.5}$ emissions and concentrations in Ontario likely resulted from changes in relative contributions by different emission sectors. Thus, improved understanding of the major sources of $PM_{2.5}$ and their contributions is vital to develop control measures and regulations to further mitigate $PM_{2.5}$ pollution and its human health effects.

Windsor is the southernmost major city in Ontario, Canada and often experiences poor air quality owing to industrial and traffic emissions and transboundary transport of air pollution from the neighboring states in the US [12]. The city reported one of the highest $PM_{2.5}$ CAAQS metric values in 2020 (i.e., 19 μg/m^3 for the 24 h CAAQS metric and 7.8 μg/m^3 for the annual metric) among the 26 stations [12]. Furthermore, Ontario's 24 h Ambient Air Quality Criteria (AAQC) was exceeded in Windsor in 2020, although both the ambient levels of $PM_{2.5}$ and its primary emissions to air have decreased over the past 10 years [10]. $PM_{2.5}$, a main smog component, remains a pollutant of concern in Windsor. As such, Windsor was selected to study potential sources of $PM_{2.5}$-bound trace elements in this border area, particularly those from local emissions and transboundary transport input. Levels of $PM_{2.5}$ and associated elements vary temporally due to changes in local meteorological conditions and emissions as well as transboundary sources [13]. Hourly measurements of trace elements collected at Windsor West station from April to October 2021 during the Michigan–Ontario Ozone Source Experiment (MOOSE) study provided finer time resolutions to improve understanding of their diurnal variability and potential sources [14].

Identifying major sources, composition, and spatial and temporal variations is important to develop effective control initiatives and air quality management strategies for $PM_{2.5}$. The source-receptor model Positive Matrix Factorization (PMF) is widely used to determine the major source categories and their contributions to ambient concentrations of $PM_{2.5}$ and its major species. The PMF can provide contributions of each source without prior information on the source profiles. By using the USEPA PMF model [15], our previous study [14] identified five source factors for the $PM_{2.5}$-bound elements in Windsor, including three traffic-related sources (vehicular exhaust, crustal dust, and vehicle tire and brake wear factors) and two industrial sources (coal/heavy oil burning and metal processing factors). The study further estimated that local traffic-related sources contributed to 47% of the total concentrations of the $PM_{2.5}$-bound elements while regional/transboundary sources contributed to the remaining 53% [14].

In our previous study [14], the input data file for the PMF model considered the following. Firstly, data below the method detection limits (MDLs) were used as-is, whereas other researchers censored input data and substituted values below MDLs with a constant value such as 1/2 MDLs [16–19]. Further research is warranted to assess if censored input data impacts identification of PMF factors and their relative contributions. Secondly, the input data file included concurrent hourly measurements of $PM_{2.5}$ and black carbon (BC), as well as calculated brown carbons (BrCs). Studies have reported that the source apportionment was sensitive to input data of $PM_{2.5}$ species concentrations, which are unique source markers [20,21]. The inclusion of organic speciation data was found to improve PMF source identification and contribution estimation of $PM_{2.5}$ in Seoul [19]. It remains to be determined if the additional BrCs data in this study enhance the source apportionment in identifying source factors of the trace elements in Windsor. Thirdly, two episodic events in 2021 were identified by examining the time series of the element concentrations. The data collected during the entire study period were included in the input data file for the PMF model to assess overall source apportionment of the trace elements in Windsor [14]. The PMF model weighed the squares of residuals with the reciprocals of the squares of the standard deviations of the data [15,22], suggesting that weight of the high concentrations was adjusted for the high concentrations. Therefore, both episodes were not well predicted by the PMF model [14]. Based on a review of the current literature, no

previous study separated episodic $PM_{2.5}$ events from the entire database to assess their unique source factors with the PMF model.

In this follow-up study, additional PMF scenarios were developed to assess if the source apportionment was sensitive to the input data: data below MDLs were replaced with 1/2 MDLs; BrCs data were excluded from the input data file; the episodic events were identified and run with the PMF model separately to investigate $PM_{2.5}$ sources and contributions; and the episodic events were further excluded from the input data file. This was intended to provide insights into how PMF model outcomes and performance were impacted by the treatment of concentrations below MDLs, exclusion of BrCs data, and exclusion of episodic events. The study further assessed unique source factors associated with the episodic events when the select data were analyzed separately.

2. Methodology

2.1. Data Collection, Screening, and Processing

During April–October 2021, hourly concentrations of $PM_{2.5}$-bound elements, $PM_{2.5}$, and BC were collected at Windsor West air monitoring station, which is located in a residential area without significant point emissions within a 2 km radius (Figure 1). Detailed information on the station and its surrounding environment can be found in our previous study [14].

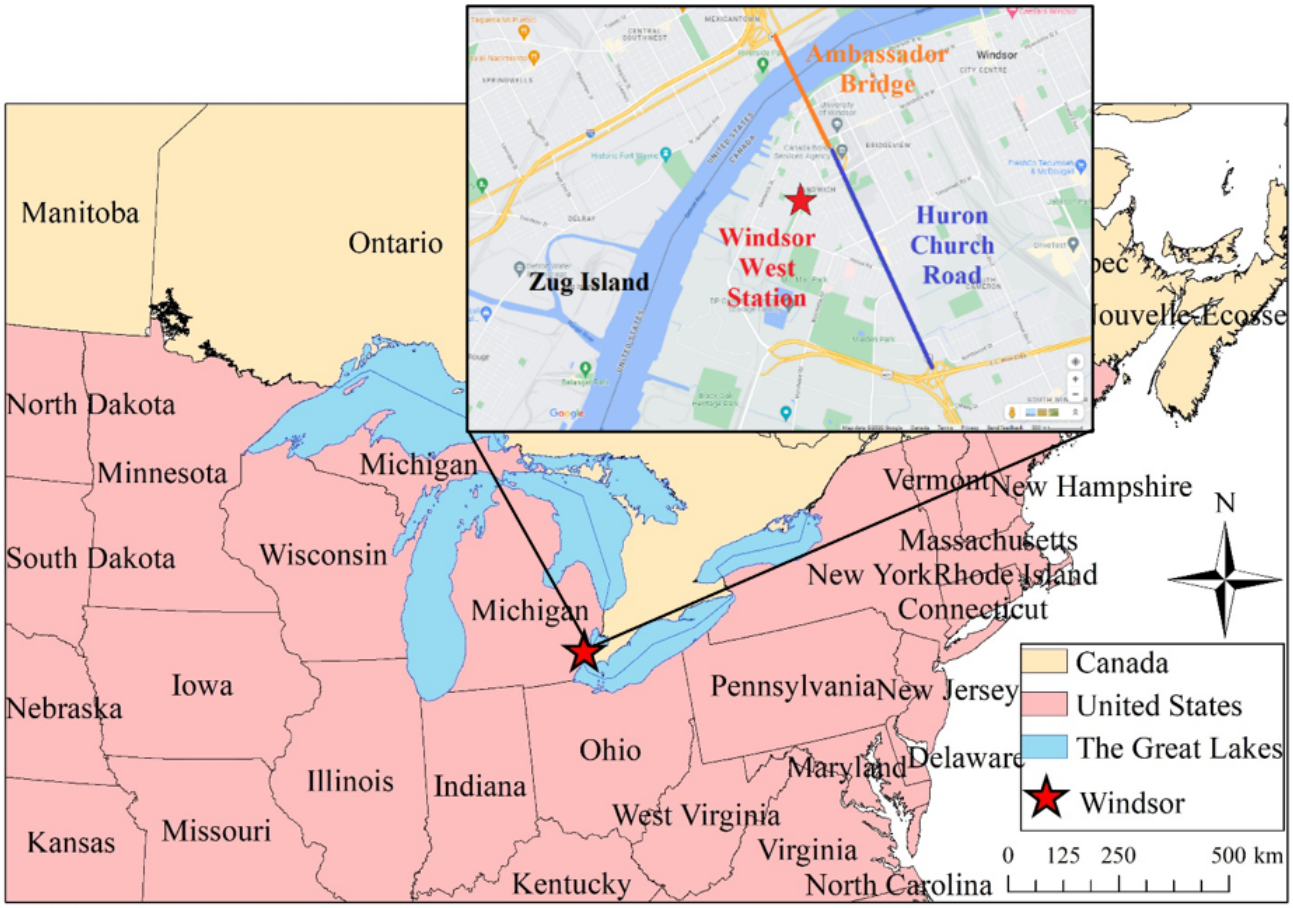

Figure 1. Location of the Windsor West air monitoring station in Ontario, Canada.

Hourly concentrations of 24 $PM_{2.5}$-bound elements (i.e., Ag, As, Ba, Br, Ca, Cd, Co, Cr, Cu, Fe, Hg, K, Mn, Ni, Pb, Rb, S, Se, Si, Sn, Sr, Ti, V, and Zn) were continuously measured by an Xact 625 particulate metal analyzer (Pall Corporation, Port Washington, NY, USA). Concentrations of hourly $PM_{2.5}$ mass were monitored by a synchronized hybrid ambient real-time particulate 5030 monitor (Thermo Fisher Scientific Corporation, Franklin,

MA, USA). In addition, hourly BC concentrations were measured by an API 633 Magee Aethalometer (Teledyne Advanced Pollution Instrumentation, Inc., San Diego, CA, USA). Brown carbon 1 (BrC_1) was estimated by subtracting BC concentrations measured at the wavelength of 370 nm from those at 520 nm. Brown carbon 2 (BrC_2) was estimated by subtracting BC concentrations measured at the wavelength of 520 nm from those at 660 nm, as reported by Sofowote et al. [23].

Detailed information of the data screening can be found in our previous paper [14]. Briefly, 8 out of the 27 species had ≥50% of their data points below MDLs (Table S1). In that study [14], data points below MDL were kept as they were; invalid or missing hourly concentrations of $PM_{2.5}$-bound elements were replaced with the median concentration of the corresponding species during the study period. In this study, additional steps were taken to process the hourly concentrations of $PM_{2.5}$-bound elements. Specifically, data points below MDLs were replaced with 1/2 MDLs for each species, as suggested by other researchers (e.g., Wang et al. [18]), and missing hourly concentrations of elements at 0:00–1:00 AM (due to instrument auto-calibration) were filled in with average concentrations of one hour before and one hour after for each element.

2.2. Design of PMF Model Scenarios

The EPA PMF5.0 model [15] was utilized to identify sources and quantify source contributions of ambient $PM_{2.5}$-bound elements. Details of PMF model settings, input data preparations, and outputs can be found in our previous study [14]. In that study, an initial PMF run was conducted using data of all 27 species collected during the entire study period, with data points below MDLs included as they were. In this follow-up study, the same PMF model settings were adopted as the initial case. Furthermore, five additional scenarios (Table 1) were developed in this study to assess whether the source apportionment by the PMF model was sensitive to the input concentration datasets. For each scenario, additional analysis was conducted, including bootstrap, displacement (DISP), and Fpeak rotation. Bootstrap was used to determine the stability of PMF solutions and the optimal number of factors, while DISP and Fpeak rotation were used to evaluate rotational ambiguity of the PMF solutions.

Table 1. Input datasets of the five different PMF scenarios.

	Scenario 1 (Base Case)	**Scenario 2**	**Scenario 3**	**Scenario 4**	**Scenario 5**
Explanatory notes for the input datasets	Replacing data below MDLs with 1/2 MDLs	Excluding BrC_1 and BrC_2	The episode on 3–5 July 2021	The episode on 20 July 2021	Excluding the two episodes
Number of samples	4362	4362	72	24	4266
Number of species	27	25	27	27	27

Scenario 1 used the dataset containing the 27 species in all samples collected during the study period; it was considered as the base case in this study. However, 8 out of 27 elements (i.e., Ag, As, Cd, Co, Cr, Rb, Sn, and V) had more than 50% of data points below MDLs (Table S1). These elements were retained in the input data because some elements are markers used for source identification, e.g., V is the marker for the factor of heavy oil burning. PMF results and performance were compared with those from our previous study [14], referred to as the initial case hereinafter, to shed light on how the treatment of data below MDLs and missing data affects the PMF model performance. BC concentrations were monitored in seven different channels during the MOOSE study. The measurements at 880 nm were reported as BC concentrations, while BrCs were calculated from those obtained at 370 nm, 520 nm, and 660 nm. Our previous study showed that BrC_1 and BrC_2 were correlated with BC (with correlation coefficients of 0.53 and 0.83, respectively), and

these three species were classified into the same PMF factor of vehicular exhaust with high loadings (72–93%). The input dataset for Scenario 2 excluded BrC_1 and BrC_2 from the input dataset of Scenario 1, to investigate whether there were benefits to including the two BrCs in the source apportionment of the $PM_{2.5}$-bound elements. If BC measurements at 880 nm wavelength were sufficient for the source apportionment, there would be little benefit to calculating BrCs from BC measurements at those additional wavelengths. By examining time series of individual elements, episodic events were identified if two criteria were met: (1) hourly concentrations were at least 12 times higher than the average concentrations during the study period for at least 2 consecutive hours in a day, and (2) multiple elements showed concurrent high hourly concentrations and exhibited similar temporal trends. A minimum of 24 consecutive samples were selected per episode to ensure sufficient sample size for PMF modeling. Two episodes were identified by using the above criteria. Concentrations of Ba, Cu, K, Rb, Sn, and Sr were high in the first episode on 3–5 July 2021 and were considered as event markers. Similarly, BrC_1, Co, Cr, Cu, Fe, Mn, and Ni were event markers for the second episode on 20 July 2021. Scenario 3 and Scenario 4 each simulated one episodic event separately. Scenario 5 excluded the two episodic events from the input dataset of Scenario 1. The results of Scenario 5 are informative as to whether excluding episodic events from the input dataset affects identification of source factors, source contributions, and model performance during the study period. Statistics of hourly concentrations for individual species are listed in Table S1 for those scenarios.

Coefficient of determination (R^2) and normalized root mean square error (NRMSE) between observed and predicted concentrations were utilized as indicators for the PMF model performance. NRMSE was calculated from a root mean square error (RMSE) divided by an observed mean concentration. The NRMSE (instead of RMSE) was chosen in this study with the following considerations: (1) observed concentrations of selected elements were much higher in the two episodic events, while their sample sizes were much smaller in comparison to the entire study period; and (2) normalizing RMSEs by observational means facilitates a fair comparison between different scenarios with various ranges of observed concentrations (Table S1).

3. Results and Discussion

3.1. PMF Scenario 1

Scenario 1 resolved an optimal five-factor solution by balancing good model performance with physical interpretability of source types. The description of factor number determination can be found in the Supplementary Materials and in Figures S1–S4. The results of Fpeak rotation and DISP suggest that there was little rotational ambiguity in the PMF solutions (Figures S5–S8). Factor names were assigned to represent their interpreted sources, including (1) coal/heavy oil burning, (2) vehicular exhaust, (3) metal processing, (4) crustal dust, and (5) vehicle tire and brake wear. The factor profiles derived by the PMF are shown in Figure 2 and Table S2 for individual elements. Details on the factor interpretation can be found in the Supplementary Materials. Table 2 shows source factors and their contributions to the $PM_{2.5}$-bound elements.

Overall, the five PMF factors resolved in the base case (i.e., Scenario 1) were consistent with those identified in the initial case from our previous study [14]. The differences in contributions of individual factors (Table 2) between the base case and the initial case were 2% or less, well within the PMF uncertainty of 10% [19]. The diurnal variations of source contributions in Scenario 1 (Figure S9) were also comparable to those in the initial case [14].

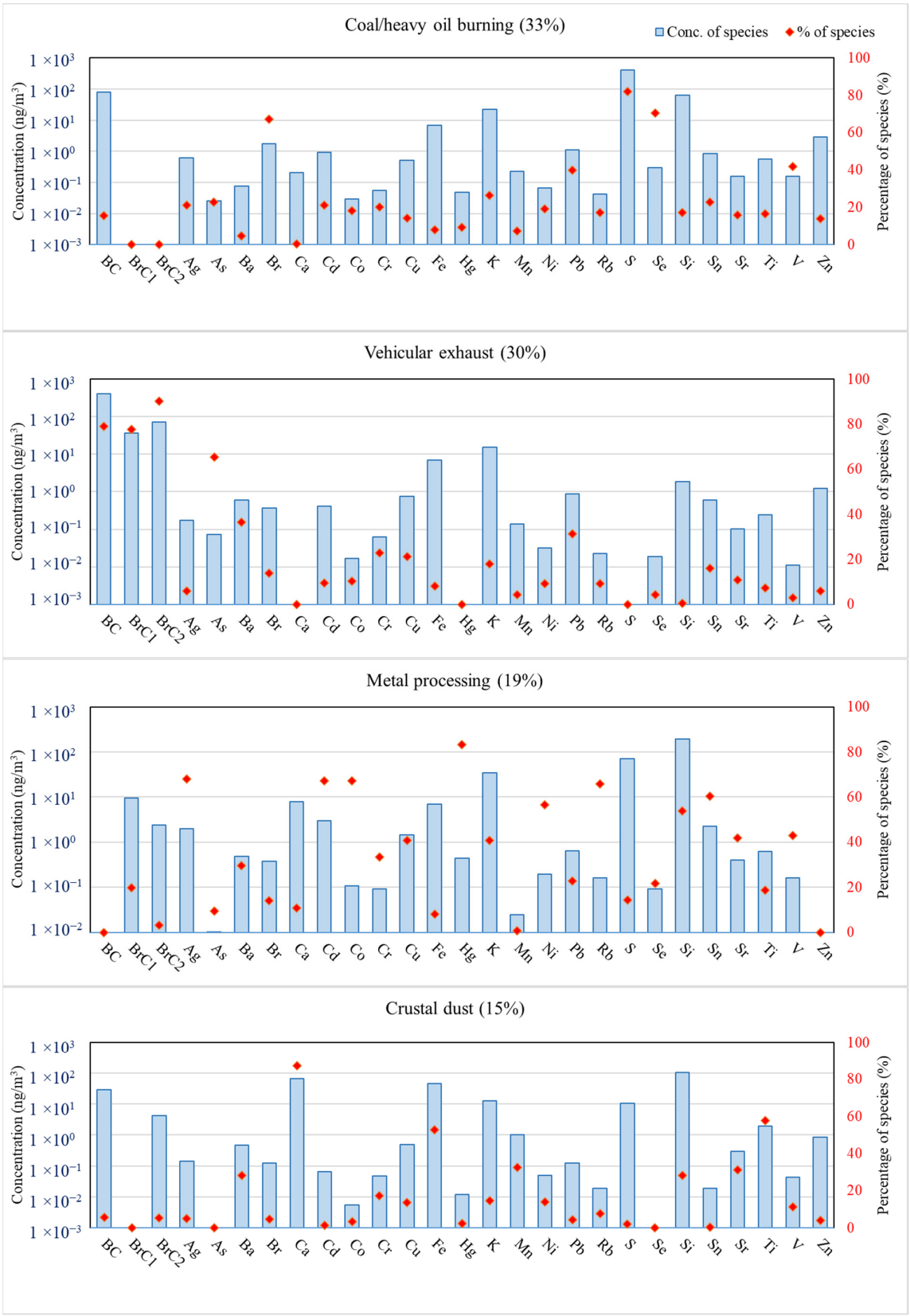

Figure 2. *Cont.*

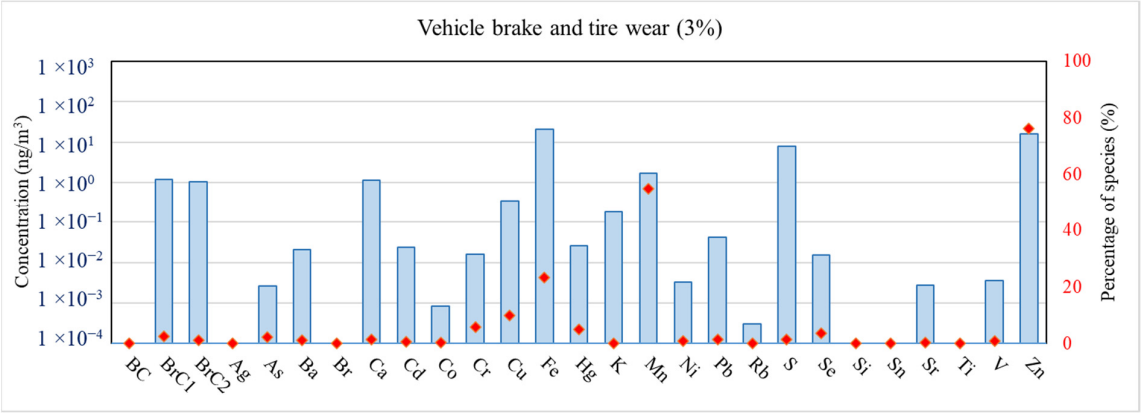

Figure 2. Profiles of five source factors identified by the PMF model for BC, BrCs, and $PM_{2.5}$-bound elements in Windsor during the study period (Scenario 1, the base case). Percentage of species (diamond symbol) shown as the secondary Y-axis is the percentage of species mass concentrations being assigned to that factor. Percentages in the subtitles are average source contributions.

Table 2. Source factors resolved by the PMF model for all scenarios and their contributions.

Factor	Initial Case (Zhang et al. [14])	Scenario 1 (Base Case)	Scenario 2 (Excluding BrC_1 and BrC_2)	Scenario 3 (The Episode on 3–5 July 2021)	Scenario 4 (The Episode on 20 July 2021)	Scenario 5 (Excluding the Two Episodes)
Coal/heavy oil burning	33%	33%	36%			34%
Vehicular exhaust	28%	30%	29%	27%	21%	30%
Metal processing	20%	19%	17%			19%
Crustal dust	16%	15%	15%		17%	14%
Vehicle tire and brake wear	3%	3%	3%			3%
Fireworks				38%		
Coal burning and metal processing				24%	22%	
Crustal dust, vehicle tire and brake wear				11%		
Heavy oil burning and metal processing					17%	
Mineral dust					23%	

The predicted total $PM_{2.5}$-bound element concentrations were in good agreement with the observed values, with an R^2 value of 0.83 (Figure S10) similar to that in the initial case (0.82). NRMSE was small (29%) and the same as in the initial case. Overall, the model performance for the base case was comparable to that in the initial case. Similar to the initial case, the PMF model was unable to accurately predict the concentrations of 14 $PM_{2.5}$-bound elements (i.e., Ag, As, Ba, Cd, Co, Cr, Cu, K, Ni, Pb, Rb, Sn, Sr, and V) ($R^2 \leq 0.2$). These elements belonged to two categories: (1) eight elements (Ag, As, Cd, Co, Cr, Rb, Sn, and V) with ≥50% of their data points below MDLs, and (2) nine elements (As, Ba, Cr, Cu, K, Ni, Pb, Sr, and V) with large variability in concentrations (coefficient of variation or CV >200%, Table S1). In all, 9 out of 14 elements (Ba, Co, Cr, Cu, K, Ni, Rb, Sn, and Sr) were classified as event markers. The low R^2 values for these nine elements were due to PMF analysis that significantly underpredicted the extremely high concentrations during the two episodic events on 3–5 July or 20 July 2021 (Figure S10). Four event markers (Co, Cr, Rb, and Sn) also had ≥50% of concentrations below MDLs. Pb was neither an event

marker nor showed ≥50% of its data points below MDLs. In other words, a higher portion of concentrations below MDLs and large variability in concentrations were the two major causes of poor model performance. In this study, the percentages of concentrations below MDLs ranged from 0% to 84% for individual, species with an average of 26%. Among the 27 species, eight (i.e., Ag, As, Cd, Co, Cr, Rb, Sn, and V) had ≥50% of their data points below MDLs. Our results suggest that replacing concentrations below MDLs with 1/2 MDLs had little effect on identifying the source factors, estimating their contributions, or PMF model performance. This finding may not be applicable to a dataset containing higher percentages of concentrations below MDLs than those in this study. In other words, replacing a higher percentage of data below MDL concentrations with 1/2 MDL could affect the PMF outcomes and performance.

3.2. PMF Scenario 2

By excluding the two BrCs from the input dataset of Scenario 1, factor profiles in Scenario 2 were largely consistent with those from the base case. The same five factors as in the base case were identified in Scenario 2, i.e., coal/heavy oil burning, vehicular exhaust, metal processing, crustal dust, and vehicular tire and brake wear (Table 2). In addition, contributions of these factors were comparable to those in the base case.

The model performance of Scenario 2 was similar to the base case. The R^2 value (0.80 vs. 0.83 in the base case) and NRMSE (30% vs. 29%) between the total predicted and total measured concentrations changed little. R^2 and NRMSE of all 25 species changed little between the two scenarios (Tables 3 and 4). Overall, excluding BrCs from the input dataset had little influence on PMF factor interpretation and model performance. In other words, BC monitoring at 880 nm wavelength is sufficient for source apportionment of trace elements in Windsor, and the BC measurements at the other wavelengths added little value.

Table 3. Coefficients of determination (R^2) of the correlations between the predicted and observed concentrations for each element in all scenarios. Elements in bold had ≥50% of their data points below MDLs in Scenario 1.

Species	Initial Case (Zhang et al. [14])	Scenario 1 (Base Case)	Scenario 2 (Excluding BrC_1 and BrC_2)	Scenario 3 (The Episode on 3–5 July 2021)	Scenario 4 (The Episode on 20 July 2021)	Scenario 5 (Excluding the Two Episodes)
BC	0.73	0.78	0.79	0.80	0.94	0.78
BrC_1	0.59	0.54		0.84	0.88	0.51
BrC_2	0.87	0.85		0.90	0.93	0.85
Ag	0.02	0.01	0.01	0.01	0.02	0.01
As	0.11	0.10	0.10	0.67	0.88	0.08
Ba	0.05	0.06	0.07	>0.99	0.95	0.19
Br	0.44	0.42	0.42	0.72	0.50	0.46
Ca	0.88	0.88	0.88	0.85	0.95	0.88
Cd	0.01	0.01	0.01	0.18	0.20	0.01
Co	0.02	0.03	0.03	0.06	0.95	<0.01
Cr	0.08	0.09	0.09	0.94	0.64	0.10
Cu	0.14	0.15	0.15	>0.99	0.88	0.40
Fe	0.36	0.35	0.35	0.92	0.77	0.62
Hg	0.23	0.23	0.24	0.01	0.72	0.21
K	0.09	0.10	0.09	>0.99	0.98	0.42
Mn	0.61	0.59	0.58	0.73	0.86	0.64
Ni	0.07	0.09	0.07	0.21	0.76	0.07
Pb	0.08	0.08	0.08	0.74	0.17	0.07
Rb	0.02	0.02	0.02	0.89	0.12	0.02

Table 3. *Cont.*

Species	Initial Case (Zhang et al. [14])	Scenario 1 (Base Case)	Scenario 2 (Excluding BrC_1 and BrC_2)	Scenario 3 (The Episode on 3–5 July 2021)	Scenario 4 (The Episode on 20 July 2021)	Scenario 5 (Excluding the Two Episodes)
S	0.70	0.72	0.69	0.95	0.44	0.71
Se	0.21	0.21	0.22	0.74	0.67	0.21
Si	0.62	0.62	0.66	0.45	0.88	0.62
Sn	0.02	0.03	0.02	0.95	<0.01	<0.01
Sr	0.03	0.03	0.03	>0.99	0.94	0.12
Ti	0.61	0.60	0.61	>0.99	0.93	0.67
V	0.06	0.05	0.05	0.10	0.82	0.05
Zn	0.85	0.86	0.87	0.47	0.75	0.87
Total elements	0.82	0.83	0.80	0.99	0.94	0.87

Table 4. NRMSE (%) between predicted and observed concentrations for each element in all scenarios. Elements in bold had ≥50% of their data points below MDLs in Scenario 1.

Species	Initial Case (Zhang et al. [14])	Scenario 1 (Base Case)	Scenario 2 (Excluding BrC_1 and BrC_2)	Scenario 3 (The Episode on 3–5 July 2021)	Scenario 4 (The Episode on 20 July 2021)	Scenario 5 (Excluding the Two Episodes)
BC 1	40	37	36	28	15	37
BrC_1	114	125		37	52	111
BrC_2	36	39		24	28	36
Ag	59	53	53	66	73	52
As	491	393	391	120	63	406
Ba	473	465	464	11	36	177
Br	60	62	62	32	93	58
Ca	54	54	53	32	13	55
Cd	48	57	57	60	41	57
Co	491	64	65	30	48	28
Cr	939	747	748	60	282	635
Cu	192	199	199	6	52	65
Fe	174	175	175	44	85	94
Hg	93	89	88	115	103	86
K	215	223	223	16	13	43
Mn	141	144	144	94	45	131
Ni	306	307	308	117	104	292
Pb	203	201	201	41	152	205
Rb	98	67	67	44	63	58
S	52	50	52	21	19	51
Se	159	157	156	50	48	158
Si	33	34	32	28	11	34
Sn	2074	104	105	43	14	23
Sr	414	426	426	12	30	138
Ti	65	66	66	13	12	58
V	258	226	226	216	68	227
Zn	96	89	85	132	55	87
Total elements	29	29	30	10	20	23

3.3. PMF Scenario 3

Scenario 3 represents the first episodic event, which occurred on 3–5 July 2021. The high concentrations of Ba, Cu, K, Rb, Sn, and Sr (Figure 3) were likely due to firework events in the surrounding US cities celebrating Independence Day. As shown in Figure 3, concentrations of all six event markers had a sharp increase from 10 PM to 11 PM on 3 July, quickly decreased at 1 AM on 4 July, and remained low during the daytime on 4 July. Afterward, elevated concentration occurred again at 11 PM on 4 July, reached peak concentration at 1 AM on 5 July, and slowly decreased until 1 PM on 5 July. Concentrations of $PM_{2.5}$ increased substantially as well, leading to a 3-day mean of 19 $\mu g/m^3$ (Table S1), which was double the average of 9 $\mu g/m^3$ observed during the study period. The firework events degraded air quality significantly due to elevated $PM_{2.5}$.

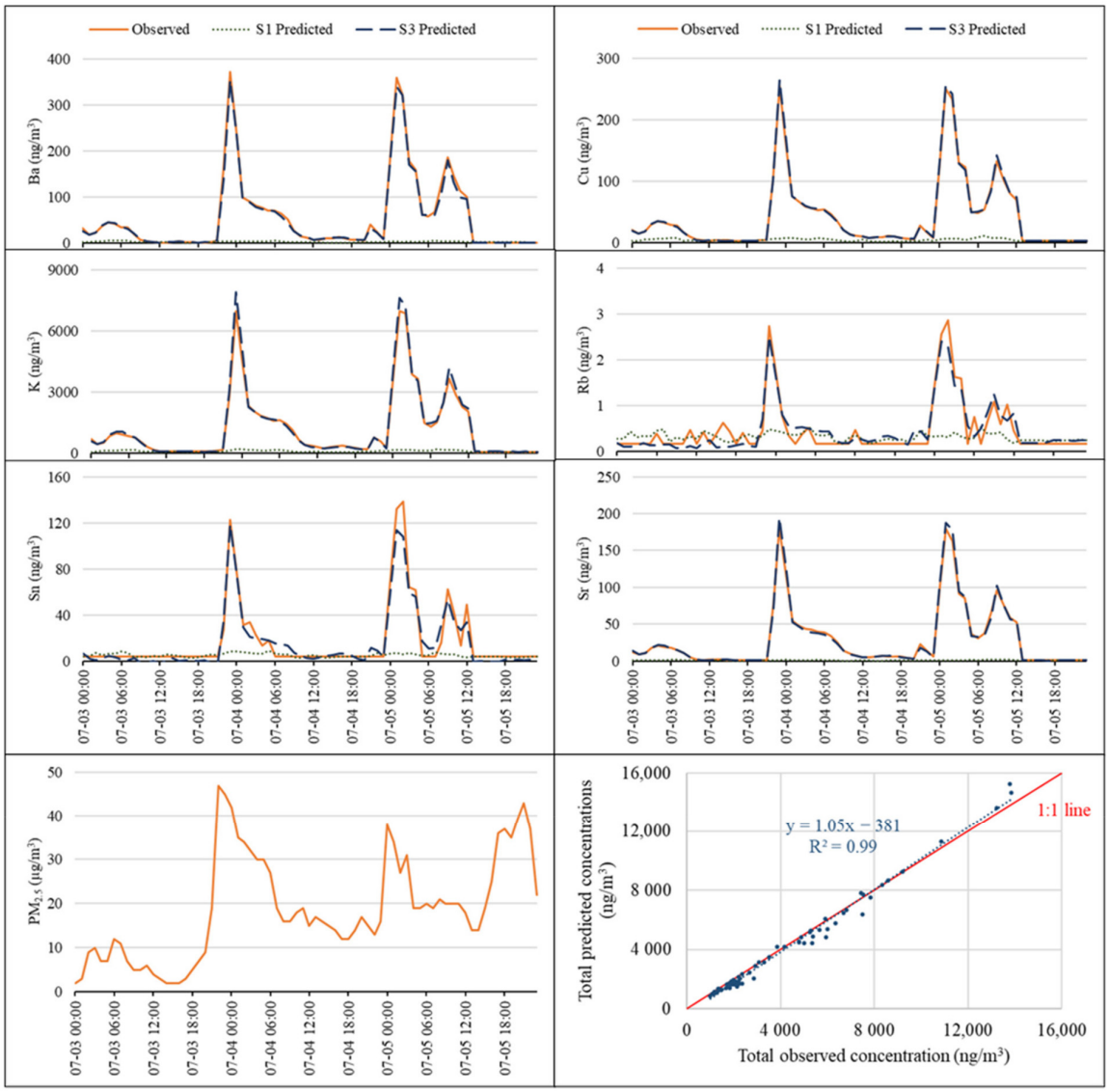

Figure 3. Time-series of hourly observed and predicted concentrations for the event markers (Ba, Cu, K, Rb, Sn, and Sr), observed $PM_{2.5}$ mass concentrations, and scatter plot of total observed and predicted concentrations of all elements during the episode on 3–5 July 2021 (Scenario 3). S1 and S3 in the figure legends correspond to Scenario 1 and Scenario 3, respectively.

In Scenario 3, the four-factor solution was deemed the best solution, based on four considerations: (1) small and stable scaled residuals (Figure S11), (2) a better goodness-of-fit by the PMF model (Figure S12), (3) one of the highest bootstrap matching rates of 98%,

indicating maximum stability of the solution (Figure S13), and (4) a good interpretability of factor profiles for the four-factor solution. Further, the four-factor solution had little rotational ambiguity due to two key reasons: (1) the number of DISP swaps was zero and the decrease in Q was less than 0.1% at any dQmax levels tested (4, 8, 15, and 25), and (2) an increase in Q-value due to the Fpeak rotation being less than 5% from the base run Q(robust). The factor profiles of Scenario 3 are shown in Table S3. In the base case, the PMF model was unable to accurately predict the peak concentrations of these elements (Figure 3). The PMF modeling for this episodic event resulted in four source factors: (1) fireworks, (2) vehicular exhaust, (3) coal/heavy oil burning and metal processing, and (4) crustal dust and brake and tire wear. The contributions of these source factors are shown in Table 2.

The factor of fireworks was the largest contributor (38%) to the total predicted concentrations of $PM_{2.5}$-bound elements. This factor was characterized by high loadings of Sn (94%), Cr (80%), Sr (75%), Ba (74%), Cu (69%), K (69%), Rb (66%), S (56%), and Ti (52%) and moderate loadings of V (30%), Se (29%), Pb (28%), and Mn (26%) (Table S3). Similar profiles of fireworks have been reported by Manchanda et al. [24], where the loadings of Ba, Sr, K, V, and S were reported as 91%, 86%, 54%, 46%, and 35%, respectively. In addition, Cu and Ti are used as color agents in fireworks to produce blue and silvery white, respectively [25]. The diurnal variability in the fireworks factor showed peak contributions at 23:00 on 3 July and 1:00–2:00 on 5 July (Figure S14). This was likely related to multiple firework events scheduled late at night in Michigan, US to celebrate Independence Day (Table S4, [26,27]). The fireworks factor likely contribute significantly (e.g., 38% in 2021) to total concentrations of $PM_{2.5}$-bound elements in early July every year due to recurring firework events in the border region.

The second-highest contributing factor was vehicular exhaust, contributing to 27% of the total concentration of $PM_{2.5}$-bound elements. The profile of this factor was similar to that of vehicular exhaust in the base case. The third-highest contributing factor was coal/heavy oil burning and metal processing, contributing to 24% of the total concentrations of $PM_{2.5}$-bound elements. This factor was characterized by high loadings of Hg (69%), Co (65%), Ag (63%), Si (59%), Ni (51%), Cd (50%), V (45%), and Se (43%) and moderate loadings of BC (38%), Ca (36%), S (35%), and Pb (28%) (Table S3). S and V are markers for coal and heavy oil burning [28,29]. Similar profiles of metal processing have been reported by Wang et al. [30], wherein loadings of Ag, Pb, Cd, Ni were 75%, 50%, 50%, and 35%, respectively. This factor was comparable to combined factors of coal/heavy oil burning and metal processing found in the base case. The factor of coal/heavy oil burning and metal processing showed a clear diurnal pattern, i.e., peaks in the nighttime and valleys in the daytime (Figure S14).

The lowest contributing factors were crustal dust and brake and tire wear, contributing to 11% of the total concentration of $PM_{2.5}$-bound elements. These factors were characterized by high loadings of Fe (65%), Mn (60%), Ca (51%), and Zn (48%) (Table S3). Ca and Fe are abundant in the earth's crust [31]. Zn and Mn are considered as major tracers of tire wear and brake wear, respectively [32,33]. These factors were comparable to the combined factors of crustal dust and brake and tire wear identified in the base case. The diurnal variability in the crustal dust and brake and tire wear factors were similar to that of vehicular exhaust (Figure S14), suggesting local emissions.

When compared with the base case, a new factor (i.e., fireworks) was identified in Scenario 3. This unique factor was the largest contributor (38%) to the total concentrations of elements during the first episodic event. This factor was not identified when the PMF model was conducted for the entire dataset. The factor of vehicular exhaust was identified in both Scenario 3 and the base case with comparable contributions (27% vs. 30%). The remaining two factors in Scenario 3 were (1) coal/heavy oil burning and metal processing, which were the combination of (a) coal/heavy oil burning and (b) metal processing factors in the base case; and (2) crustal dust and brake and tire wear, which were the grouping of (a) crustal dust and (b) brake and tire wear factors in the base case. Because the number of factors was reduced to four in Scenario 3 and a new factor of fireworks was identified, the

factors of coal/heavy oil burning and metal processing factors in Scenario 1 merged into a single factor in Scenario 3, and factors of brake and tire wear and crustal dust also became a single factor.

By extracting the data in the first episodic event on 3–5 July 2021, the PMF modeling yielded a much better performance. This was reflected by a much higher R^2 value (0.99 vs. 0.83, Table 3) and a much lower NRMSE (10% vs. 29%, Table 4) between the total predicted and observed concentrations when compared to those in the base case. For individual elements, R^2 and NRMSE values were improved for all six event markers (i.e., Ba, Cu, K, Rb, Sn, and Sr). As shown in Figure 3, the model–measurement agreement was excellent for both high and low concentrations in Scenario 3, compared with significantly underestimated concentrations in Scenario 1 (also see ratio plots in Figure S15). The improvement in model performance for the six event markers was attributed to the identification of the unique source factor of fireworks that was not identified in the base case when all data were included (Figure 3 and Table S3). The loadings of the six event markers were relatively high, ranging from 66–94% (Table S3). It should be noted that 58% of Sn concentrations were below MDLs, but these acted as an event marker. Improved R^2 and NRMSE values were also observed for eight additional elements. Six of them had significantly lower variability in observed concentrations in Scenario 3 than those in Scenario 1, i.e., As (165% vs. 396% in the base case), BrC_1 (89% vs. 154%), Cr (179% vs. 757%), Fe (131% vs. 209%), Pb (80% vs. 207%), and Se (93% vs. 167%). For the other two elements, variabilities in observed concentrations in Scenario 3 were slightly lower than those in Scenario 1, i.e., Br (58% vs. 79%) and Ti (101% vs. 108%). Zn was the only element showing reduced R^2 (0.47 vs. 0.86) and increased NRMSE (132% vs. 89%). This was partially due to greater underestimation of the observed concentration of 320 ng/m^3 at 7 AM on 5 July in Scenario 3 (63 ng/m^3) than that in Scenario 1 (225 ng/m^3), as shown in Figure S16. There was little change in R^2 and NRMSE for the remaining 12 elements (BC, BrC_2, Ag, Ca, Cd, Co, Hg, Mn, Ni, S, Si, and V).

Overall, the model performance in Scenario 3 was greatly improved, as indicated by higher R^2 values and lower NRMSE for the total concentrations and for 14 out of the 27 individual elements. Therefore, running the PMF model for an episodic event not only identifies unique sources, but also greatly improves the PMF model performance. This would lead to better source identification and improved quantification of source contributions. In the future, PMF source apportionment studies challenged with poor model performance due to elevated concentrations in a short time period may consider analyzing episodic events separately to identify unique sources associated with the episodes and to improve model performance.

3.4. PMF Scenario 4

Scenario 4 is the second episodic event, which occurred on 20 July 2021, with elevated concentrations of BrC_1, Co, Cr, Cu, Fe, Mn, and Ni (Figure 4). Concentrations of all seven event markers, except for Mn, started to increase around 2–3 AM on 20 July, reached peak values at 4–6 AM, and then decreased at 7–8 AM, remaining low for the rest of the day (Figure 4). Concentrations of Mn were high at 1 AM on 20 July and slowly decreased afterwards. The $PM_{2.5}$ concentrations were also elevated, with a daily mean of 23 μg/m^3 (Table S1), more than double the average concentration of 9 μg/m^3 during the study period.

In Scenario 4, two-, three-, and four-factor solutions had higher bootstrap mapping rates of 80–87% than in other solutions (Figure S17). In addition, the DISP results showed that the number of swaps was zero at any dQmax level (4, 8, 15, and 25) and the decrease in Q was less than 0.1% for two-, three-, four-, and five-factor solutions. However, the five-factor solution had smaller and more stable scaled residuals of elements as reflected, respectively, in IM and IS (Figure S18); a better goodness-of-fit by the model, i.e., smaller Q(robust) and Q(true) (Figure S19); and a good interpretability of factor profiles. As for the Fpeak rotation, increases in Q-value due to the Fpeak rotation were more than 5% from the base run Q(robust) for two-, three-, four-, and five-factor solutions, i.e., a sign of rotational

ambiguity in the PMF solutions. This was likely because of the small sample size (24) in Scenario 4 when compared with the number of variables (27), as pointed out by other studies [34]. As such, the five-factor solution was selected in Scenario 4.

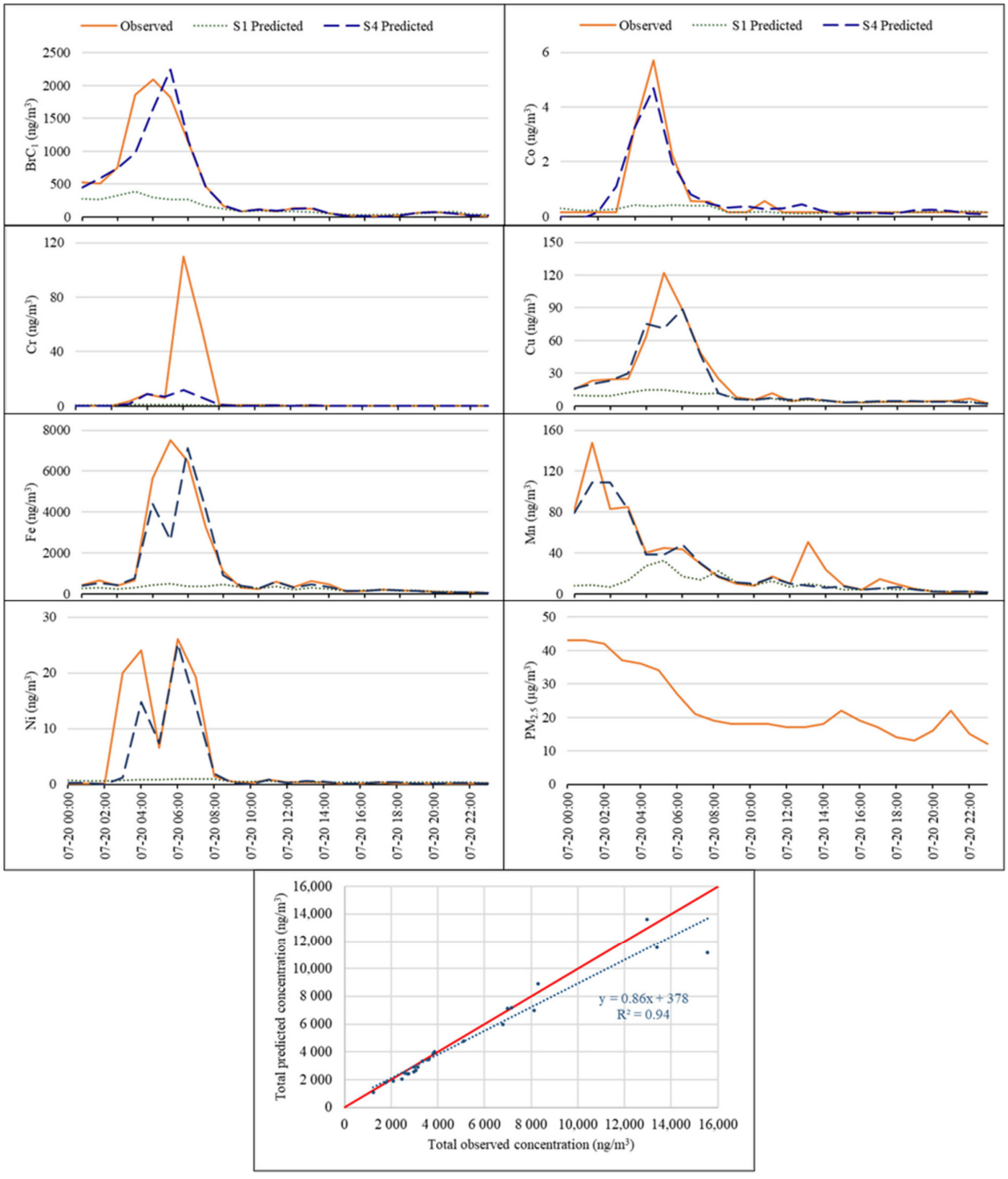

Figure 4. Time-series of hourly observed and predicted concentrations for the event markers (BrC_1, Co, Cr, Cu, Fe, Mn, and Ni), observed $PM_{2.5}$ mass concentrations, and scatter plot of total observed and predicted concentrations of all elements during the episode on 20 July 2021 (Scenario 4). S1 and S4 in the figure legends correspond to Scenario 1 and Scenario 4, respectively.

The factor profiles of Scenario 4 are shown in Table S5. The PMF modeling resulted in five source factors: (1) mineral dust, (2) coal burning and metal processing, (3) vehicular exhaust and tire wear, (4) heavy oil burning and metal processing, and (5) crustal dust. The contributions of these source factors are shown in Table 2.

The factor of mineral dust was the largest contributor (23%) to the total predicted concentration of $PM_{2.5}$-bound elements during the second episodic event. This factor was characterized by high loadings of Ba (71%), Mn (62%), Sr (59%), and K (46%) and moderate loadings of BC (33%) and Ti (31%) (Table S5). Similar profiles of mineral dust have been reported by Liu et al. [35], with loadings of Ba, Mn, K, and Ti reported as 55%, 40%, 40%, and 25%, respectively. There are 37 active mines in Ontario [36], two iron mines in Michigan [37], and 75 active coal-mining operations in Ohio [38]. During this episode on 20 July 2021, the average wind speed was 6.6 km/h at Windsor West station. In 17 out of 24 h, the winds blew from the west (220°–290°), where Zug Island in Michigan is located (Figure 1). Zug Island is a heavily industrialized area that produces coke and processes metals [39]. Air masses in the remaining seven hours were from the south and north. The hourly contributions of the mineral dust source factor varied greatly from 2500 ng/m^3 at 5:00 AM to 270 ng/m^3 at 23:00 (Figure S20). The high values above the daily average of 1100 ng/m^3 were associated with air masses from the south and west (190–300°, Figure S21), suggesting that the mineral dust factor was strongly influenced by transboundary sources.

The second-highest contributing factor was coal burning and metal processing, which accounted for 22% of the total predicted concentration of $PM_{2.5}$-bound elements. This factor was characterized by high loadings of Ag (67%), Cd (63%), Sn (58%), S (54%), Rb (51%), and Si (44%), moderate loadings of K (32%), Br (32%), and Se (31%), and low loadings of Co (17%) and V (16%) (Table S5). Similar factor profiles of metal processing have been reported by Wang et al. [30], i.e., Ag (75%), Cd (50%), Rb (30%), K (20%), and V (20%). S is the marker for coal combustion [28]. In addition, the factor profiles are similar to those profiles of coal combustion reported by Sugiyama et al. [40], i.e., Cd (65%), Sn (50%), Co (20%), and V (16%).

The next two contributing factors were vehicular exhaust and crustal dust, each of which contributed 21% and 17%, respectively, of the total concentrations of $PM_{2.5}$-bound elements. The profiles of the two factors were similar to the profile of vehicular exhaust and crustal dust in the base case. The least-contributing factor was heavy oil burning and metal processing (17%), which was characterized by high loadings of Ni (82%), Hg (69%), Fe (61%), Cr (54%), and V (45%) and moderate loadings of As (37%) and Pb (25%) (Table S5). The profile is similar to that of metal manufacturing reported by Liu et al. [41], i.e., Ni (50%), Fe (40%), Cr (40%), and As (35%); and by Wang et al. [30], i.e., Pb (50%), As (45%), Ni (30%), Cr (30%), and V (20%). V is also considered as a marker for heavy oil burning [29].

When compared with the base case, a new factor (i.e., mineral dust) was identified in Scenario 4. This factor was the largest contributor (23%) to the total concentration of $PM_{2.5}$-bound elements during the episode. This factor did not emerge when the PMF modeling was run with the full dataset. The factors of vehicular exhaust and crustal dust were identified in both Scenario 4 and the base case, and the contributions were comparable (Table 2). The remaining two factors for Scenario 4 were (1) coal burning and metal processing and (2) heavy oil burning and metal processing, respectively, with a narrower range of source contributions (17–22%) when compared with that of 19–33% (coal/heavy oil burning and metal processing) in the base case.

By selecting data in the second episodic event on 20 July 2021, the PMF modeling yielded a much better performance relative to the base case, with a higher R^2 value (0.94 vs. 0.83) and a lower NRMSE (20% vs. 29%). As seen in Figure 4, the predicted concentrations tracked observed concentrations well in Scenario 4 for all seven event markers (BrC_1, Co, Cr, Cu, Fe, Mn, and Ni), whereas the predicted concentrations were highly underestimated in Scenario 1 (also see ratio plots in Figure S22). Consequently, R^2 and NRMSE values were improved. It should be noted that Co and Cr each had ≥50% of their data points below MDLs, but acted as event markers. The improvement in R^2 and NRMSE was also observed for six more elements with significantly lower variability in concentrations, i.e., As (175% vs. 396%), Ba (141% vs. 470%), K (78% vs. 229%), Se (82% vs. 167%), Sr (117% vs. 429%), and Ti (47% vs. 108%). Significant improvement in R^2 was also found for Hg (0.72 vs. 0.23) and V (0.82 vs. 0.05). This is likely because peak concentrations (i.e., at

3–6 AM on 20 July) of those elements were better predicted in Scenario 4 than in Scenario 1 (Figure S23). However, S experienced a worse R^2 (0.44 vs. 0.72) but a better NRMSE (19% vs. 50%). Predicted S concentrations were underestimated, further deviating from the observed values in Scenario 4 than those in Scenario 1.

Overall, the model performance in Scenario 4 was greatly improved for total elemental concentrations and 15 out of the 27 elements, with higher R^2 values and lower NRMSE than those in the base case, suggesting better identified source factors and improved quantification of source contributions. The findings once again suggest that analyzing the episodic event separately is beneficial to identify unique sources related to the episode, e.g., transboundary sources of mineral dust from the south and west directions.

3.5. PMF Scenario 5

By removing the two episodes which occurred on 3–5 July and 20 July from the dataset, Scenario 5 resulted in the same five factors as in the base case (Table 2). The factor profiles and contributions in Scenario 5 were almost identical to those obtained from the base case (Table 2, Tables S2, S6 and S7).

The PMF model performance of Scenario 5 was slightly improved when compared with the base case. This was reflected by an increased R^2 value from 0.83 to 0.87 (Table 3) and a decreased NRMSE (23% vs. 29%, Table 4). Specifically, R^2 and NRMSE were improved for the event markers of Cu and K in the first episode and Fe in the second episode. This was largely attributed to the reduced variability in concentrations for Cu (81% vs. 209%), K (55% vs. 225%), and Fe (143% vs. 209%), when the elevated concentrations of these event markers (Table S1) were excluded in Scenario 5. The model performance for the remaining 24 elements changed little.

Overall, excluding the two episodic events had little impact on identifying source factors and estimating their contributions (Table 2). This could be due to the small sample size of the two episodic events (n = 72 in Scenario 3 and n = 24 in Scenario 4) relative to the entire dataset (n = 4362). However, the PMF model performance in Scenario 5 was slightly improved for 3 out of 12 event markers (Tables 3 and 4) in comparison to the base case, with the much better fit of the predicted concentrations to the observed concentrations attributed to decreased variability in concentrations. This suggests that the PMF model has difficulty in predicting a few exceptionally high values when the variability in concentrations is large due to episodic events.

4. Conclusions

Our previous source apportionment study with the PMF model resulted in five source factors: (1) coal/heavy oil burning, (2) vehicular exhaust, (3) metal processing, (4) crustal dust, and (5) vehicle tire and brake wear [14]. Model performance was good for total concentrations but less satisfactory for elements with elevated concentrations in the two episodic events and for elements with $\geq$50% of their data below MDLs. In this study, five scenarios were devised to investigate whether there were benefits to the PMF model outcome and performance by (1) replacing concentrations below MDLs with 1/2 MDLs (Scenario 1), (2) excluding BrCs data from the input data (Scenario 2), (3) analyzing episodic events separately (Scenarios 3 and 4), and (4) excluding the two episodic events (Scenario 5). PMF source factors, source contributions, and model performance (indicated by R^2 and NRMSE) were compared between the initial case and Scenario 1; and between Scenario 1 and each of Scenarios 2, 3, 4, and 5.

By replacing data below MDL with 1/2 MDL, the same five PMF factors were resolved in Scenario 1. Factor profiles and source contributions in Scenario 1 were largely consistent with those in the initial case [14]. Our results indicate that the replacement of data below MDLs with 1/2 MDLs in PMF source apportionment had little effect on source identification, estimating source contributions, or model performance. If a dataset contains higher percentages of data below MDLs than this study (range: 0–84%, average: 26%, 8 out of

27 elements had ≥50% of their data points below MDLs), dealing with data below MDLs may affect the PMF outcomes and performance.

By excluding BrCs concentrations from the input dataset in Scenario 1, the same five PMF factors were identified, and source contributions and model performance were largely comparable with those in Scenario 1. As such, BC measurements are sufficient and BrCs had little added value to source apportionment of $PM_{2.5}$-bound elements.

By extracting data from episodic events and conducting PMF source apportionment for each event, one unique factor of fireworks for the first episode (Scenario 3) and another unique factor of mineral dust from the second episode (Scenario 4) were identified. Neither of these source factors were observed in Scenario 1. Furthermore, model performance was greatly improved in Scenarios 3 and 4 for event markers and additional elements, with less variability in concentrations. This indicates that analyzing episodic events separately is beneficial to identifying new source factors, thus improving source contribution estimates and model performance. Further, the widespread wildfire smoke in Spring 2023 in North America [42] highlights the need to investigate $PM_{2.5}$ sources and contributions during episodic events. The inherited rotational ambiguity due to a small sample size during episodic events could be resolved by increasing the sample size.

Compared with Scenario 1, exclusion of the two episodic events from the dataset (Scenario 5) resulted in the same five source factors, similar source contributions, and slightly improved model performance, especially for 3 out of 12 event markers. However, the benefit was limited, due to the small sample size of the episodic events (n = 96 total) when compared with the entire dataset (n = 4362).

In summary, replacing data points below MDLs with 1/2 MDL or excluding BrCs in input data has little impact on source identification, source contribution, and model performance for apportionment of $PM_{2.5}$-bound elements. However, the model outcomes and performance are highly sensitive to episodic events. Modeling the episodic events separately not only identified unique sources associated with the events, but also significantly improved model performance, although the occurrence of these events was less frequent. On the other hand, excluding the two episodic events from the dataset did not change the model outcomes much and the improvement in model performance was limited to a few event markers. The analysis of elements with poor or significantly improved model performance suggests that the PMF model outcomes and performance are sensitive to percentages of data below MDLs and concentrations with large variability, such as infrequent occurrence of extremely high values. The latter could be resolved by analyzing episodic events separately. As for the large percentage of concentrations below MDLs, including those elements in PMF analysis will likely degrade the model performance and may introduce large uncertainty to source factors and their contributions. On the other hand, some of those elements could act as event markers in episodes with high concentrations, leading to identification of unique source factors. Researchers should consider the benefits of including more elements and the drawbacks of a large percentage of concentrations below MDLs.

Our findings can guide future source apportionment analysis using the PMF model, especially when the dataset contains data points below MDLs or episodic events. Future studies should investigate the sensitivity of PMF source apportionment of ambient $PM_{2.5}$-bound elements to input concentration data at other locations and with longer study periods.

Supplementary Materials: The following supporting information can be downloaded at: https://www.mdpi.com/article/10.3390/atmos14081269/s1, Figure S1: IM and IS vs. number of factors in Scenario 1. Figure S2: Q(Robust) and Q(True) vs. number of factors in Scenario 1. Figure S3: Q/Qexp vs. number of factors in Scenario 1. Figure S4: The percentage of bootstrap matching vs. number of factors in Scenario 1. Figure S5: Factor contributions (ng/m^3 and %) of BC to individual PMF resolved sources (factor contribution >0.05% is shown) at Fpeak strength of −1, −0.5, 0.5, and 1 in the base model (Run 15) of Scenario 1. Factor 1: Crustal dust, Factor 2: Coal/heavy oil burning, Factor 3: Vehicular exhaust. Figure S6: Factor contributions (ng/m^3 and %) of BrC1 to individual PMF resolved sources (factor

contribution >0.05% is shown) at Fpeak strength of −1, −0.5, 0.5, and 1 in the base model (Run 15) of Scenario 1. Factor 3: Vehicular exhaust, Factor 4: Metal processing, Factor 5: Vehicle tire and brake wear. Figure S7: Factor contributions (ng/m^3 and %) of BrC2 to individual PMF resolved sources (factor contribution >0.05% is shown) at Fpeak strength of −1, −0.5, 0.5, and 1 in the base model (Run 15) of Scenario 1. Factor 1: Crustal dust, Factor 2: Coal/heavy oil burning, Factor 3: Vehicular exhaust, Factor 4: Metal processing, Factor 5: Vehicle tire and brake wear. Figure S8: Factor contributions (ng/m^3 and %) of Pb to individual PMF resolved sources (factor contribution >0.05% is shown) at Fpeak strength of −1, −0.5, 0.5, and 1 in the base model (Run 15) of Scenario 1. Factor 1: Crustal dust, Factor 2: Coal/heavy oil burning, Factor 3: Vehicular exhaust, Factor 4: Metal processing, Factor 5: Vehicle tire and brake wear. Figure S9: Diurnal variations in PMF estimated source contributions (ng/m^3) in Scenario 1 (percentages in the subtitles are average source contributions) and total concentrations of all factors, and observed $PM_{2.5}$ concentration (μg/m^3). Figure S10: Scatter plot of hourly total observed vs. predicted concentrations (Scenario 1). The two episodes are labelled in red and green, respectively. When concentrations were greater than 4000 ng/m^3, most of the hourly concentrations in the two episodes deviated further away from the 1:1 line. Figure S11: IM and IS vs. number of factors in Scenario 3. Figure S12: Q(Robust) and Q(True) vs. number of factors in Scenario 3. Figure S13: The percentage of bootstrap matching vs. number of factors in Scenario 3. Figure S14: Time-series of PMF estimated factor concentrations (ng/m^3) in Scenario 3 (percentages in the subtitles are average source contributions) and total concentrations of all factors, and observed $PM_{2.5}$ concentration (μg/m^3). Figure S15: Ratios of observed to predicted concentrations for event markers in Scenarios 1 and 3 vs. observed concentrations. Figure S16: Time-series of hourly observed and predicted concentrations for As, BrC1, Br, Cr, Fe, Pb, Se, Ti, and Zn during the episode on 3–5 July 2021 (Scenario 3). S1 and S3 in the figure legends correspond to Scenario 1 and Scenario 3, respectively. Figure S17: The percentage of bootstrap matching vs. number of factors in Scenario 4. Figure S18: IM and IS vs. number of factors in Scenario 4. Figure S19: Q(Robust) and Q(True) vs. number of factors in Scenario 4. Figure S20: Time-series of PMF estimated factor concentrations (ng/m^3) in Scenario 4 (percentages in the subtitles are average source contributions) and total concentrations of all factors, and observed $PM_{2.5}$ concentration (μg/m^3). Figure S21: Source contributions of the mineral dust factor in Scenario 4 vs. hourly wind direction on 20 July 2021. Figure S22: Ratios of observed to predicted concentrations for event markers in Scenarios 1 and 4 vs. observed concentrations. Figure S23: Time-series of hourly observed and predicted concentrations for As, Ba, K, Se, Sr, and V during the episode on 20 July 2021 (Scenario 4). S1 and S4 in the figure legends correspond to Scenario 1 and Scenario 4, respectively. Table S1: Statistics of hourly concentrations for $PM_{2.5}$, BC and BrCs (μg/m^3), and $PM_{2.5}$-bound elements (ng/m^3) during April–October 2021. Table S2: Factor profiles (% of species mass concentrations being assigned to that factor) for black carbon (BC) and brown carbons (BrC1 and BrC2), and $PM_{2.5}$-bound elements in Windsor during April–October 2021 (Scenario 1). Bold values are percentages ≥40%. Table S3: Factor profiles (% of species mass concentrations being assigned to that factor) for black carbon (BC) and brown carbons (BrC1 and BrC2), and $PM_{2.5}$-bound elements in Windsor during the 1st episodic event on 3–5 July 2021 (Scenario 3). Bold values are percentages ≥40%. Table S4: List of firework events in Michigan in July 2021 (Data sources: Oilver [23]; Mlive [24]). Table S5: Factor profiles (% of species mass concentrations being assigned to that factor) for black carbon (BC) and brown carbons (BrC1 and BrC2), and $PM_{2.5}$-bound elements in Windsor during the 2nd episodic event on 20 July 2021 (Scenario 4). Bold values are percentages ≥40%. Table S6: Factor profiles (% of species mass concentrations being assigned to that factor) for black carbon (BC) and brown carbons (BrC1 and BrC2), and $PM_{2.5}$-bound elements in Windsor, excluding the two episodic events (Scenario 5). Bold values are percentages ≥40%. Table S7: Vehicle exhaust factor profiles (% of species mass concentrations being assigned to that factor) in each of the five scenarios. Bold values are percentages ≥40%. References [14,16,18,19,26–33,40,43–53] are cited in Supplementary Materials.

Author Contributions: Conceptualization, methodology, and supervision, Y.S. and X.X.; data curation, J.D., M.N. and A.M.; formal analysis and visualization, T.Z.; writing—original draft preparation, T.Z., Y.S. and X.X.; writing—review and editing, T.Z., Y.S. and X.X.; funding acquisition, Y.S. and X.X. All authors have read and agreed to the published version of the manuscript.

Funding: This research was funded by Environment and Climate Change Canada, the Natural Sciences and Engineering Research Council of Canada, and University of Windsor's Ignite Program.

Institutional Review Board Statement: Not applicable.

Informed Consent Statement: Not applicable.

Data Availability Statement: The following datasets are publicly available and can be downloaded from government websites. Hourly concentrations of $PM_{2.5}$, black carbons, and $PM_{2.5}$-bound elements between April and October 2021 are available upon request from the corresponding author or at the repository for the MOOSE study: https://www-air.larc.nasa.gov/missions/moose/index.html (accessed on 10 February 2023).

Acknowledgments: We would like to acknowledge Don Bourne at the University of Windsor for his editorial assistance, and Chris Charron at the Ontario Ministry of the Environment, Conservation, and Parks for his management support with participation in the MOOSE study.

Conflicts of Interest: The authors declare no conflict of interest.

References

1. Dabek-Zlotorzynska, E.; Dann, T.F.; Kalyani Martinelango, P.; Celo, V.; Brook, J.R.; Mathieu, D.; Ding, L.; Austin, C.C. Canadian National Air Pollution Surveillance (NAPS) $PM_{2.5}$ speciation program: Methodology and $PM_{2.5}$ chemical composition for the years 2003–2008. *Atmos. Environ.* **2011**, *45*, 673–686.
2. Jeong, C.H.; Traub, A.; Huang, A.; Hilker, N.; Wang, J.M.; Herod, D.; Dabek-Zlotorzynska, E.; Celo, V.; Evans, G.J. Long-term analysis of $PM_{2.5}$ from 2004 to 2017 in Toronto: Composition, sources, and oxidative potential. *Environ. Pollut.* **2020**, *263*, 114652.
3. Tchounwou, P.B.; Yedjou, C.G.; Patlolla, A.K.; Sutton, D.J. Heavy metal toxicity and the environment. *Mol. Clin. Environ. Toxicol.* **2012**, *101*, 133–164.
4. Health Canada (HC). *Canadian Health Science Assessment for Fine Particulate Matter (PM2.5)*; Health Canada (HC): Ottawa, ON, Canada, 2022; ISBN 978-0-660-41742-4.
5. Environment and Climate Change Canada (ECCC). Criteria Air Contaminants. 2017. Available online: https://www.ec.gc.ca/air/default.asp?162lang=En&n=7C43740B-1 (accessed on 20 July 2023).
6. United States Environmental Protection Agency (USEPA). Criteria Air Pollutants. 2023. Available online: https://www.epa.gov/criteria-air-pollutants (accessed on 20 July 2023).
7. CCME. *Guidance Document on Achievement Determination Canadian Ambient Air Quality Standards for Fine Particulate Matter and Ozone*; Canadian Council of Ministers of the Environment: Winnipeg, MB, Canada, 2012; ISBN 978-1-896997-91-9.
8. Government of Canada. Canadian Environmental Protection Act. 1999. Available online: www.canada.ca/en/environment-climate-change/services/canadian-environmental-protection-act-registry/related-documents.html (accessed on 20 July 2023).
9. Ministry of the Environment, Conservation and Parks (MECP). Air Quality Health Index and Air Quality Alert. 2019. Available online: https://www.ontario.ca/document/air-quality-ontario-2015-report/air-quality-health-index-and-air-quality-alerts#:~:text=On%20June%2024%2C%202015%2C%20in,the%20foundation%20of%20the%20AQI%20 (accessed on 4 July 2023).
10. Ministry of the Environment, Conservation and Parks (MECP). Air Quality in Ontario 2020 Report. 2022. Available online: https://www.ontario.ca/document/air-quality-ontario-2020-report (accessed on 4 July 2023).
11. World Health Organization (WHO). Ambient (Outdoor) Air Pollution. 2023. Available online: https://www.who.int/news-room/fact-sheets/detail/ambient-(outdoor)-air-quality-and-health#:~:text=The%20WHO%20Global%20air%20quality,%2Dbased%20decision%2Dmaking%20process (accessed on 4 July 2023).
12. MECP. Air Quality in Ontario 2020 Report. 2023. Available online: https://www.ontario.ca/document/air-quality-ontario-2020-report (accessed on 20 May 2023).
13. Sofowote, U.M.; Di Federico, L.M.; Healy, R.M.; Debosz, J.; Su, Y.; Wang, J.; Munoz, A. Heavy metals in the near-road environment: Results of semi-continuous monitoring of ambient particulate matter in the greater Toronto and Hamilton area. *Atmos. Environ. X* **2019**, *1*, 100005.
14. Zhang, T.; Su, Y.; Debosz, J.; Noble, M.; Munoz, A.; Xu, X. Continuous Measurements and Source Apportionment of Ambient $PM_{2.5}$-Bound Elements in Windsor, Canada. *Atmosphere* **2023**, *14*, 374. [CrossRef]
15. United States Environmental Protection Agency (USEPA). EPA Positive Matrix Factorization (PMF) 5.0 Fundamentals and User Guide. 2014. Available online: https://www.epa.gov/sites/default/files/2015-02/documents/pmf_5.0_user_guide.pdf (accessed on 20 May 2023).
16. Pekney, N.J.; Davidson, C.I.; Robinson, A.; Zhou, L.; Hopke, P.; Eatough, D.; Rogge, W.F. Major Source Categories for $PM_{2.5}$ in Pittsburgh using PMF and UNMIX. *Aerosol Sci. Technol.* **2006**, *40*, 910–924.
17. Juda-Rezler, K.; Reizer, M.; Maciejewska, K.; Błaszczak, B.; Klejnowski, K. Characterization of atmospheric $PM_{2.5}$ sources at a Central European urban background site. *Sci. Total Environ.* **2020**, *713*, 136729. [CrossRef]
18. Wang, H.; Zhang, L.; Cheng, I.; Yao, X.; Dabek-Zlotorzynska, E. Spatiotemporal trends of $PM_{2.5}$ and its major chemical components at urban sites in Canada. *J. Environ. Sci.* **2021**, *103*, 1–11. [CrossRef]
19. Shin, S.M.; Kim, J.Y.; Lee, J.Y.; Kim, D.S.; Kim, Y.P. Enhancement of modeling performance by including organic markers to the PMF modeling for the $PM_{2.5}$ at Seoul. *Air Qual. Atmos. Health* **2022**, *15*, 91–104.

20. Xie, M.; Hannigan, M.P.; Dutton, S.J.; Milford, J.B.; Hemann, J.G.; Miller, S.L.; Schauer, J.J.; Peel, J.L.; Vedal, S. Positive matrix factorization of $PM_{2.5}$: Comparison and implications of using different speciation data sets. *Environ. Sci. Technol.* **2012**, *46*, 11962–11970.
21. Li, W.; Qi, Y.; Qu, W.; Qu, W.; Shi, J.; Zhang, D.; Liu, Y.; Zhang, Y.; Zhang, W.; Ren, D.; et al. $PM_{2.5}$ source apportionment identified with total and soluble elements in positive matrix factorization. *Sci. Total Environ.* **2023**, *858*, 159948. [PubMed]
22. Lee, E.; Chan, C.K.; Paatero, P. Application of positive matrix factorization in source apportionment of particulate pollutants in Hong Kong. *Atmos. Environ.* **1999**, *33*, 3201–3212.
23. Sofowote, U.M.; Healy, R.M.; Su, Y.; Debosz, J.; Noble, M.; Munoz, A.; Jeong, C.-H.; Wang, J.M.; Hilker, N.; Evans, G.J.; et al. Understanding the $PM_{2.5}$ imbalance between a far and near-road location: Results of high temporal frequency source apportionment and parameterization of black carbon. *Atmos. Environ.* **2018**, *173*, 277–288.
24. Manchanda, C.; Kumar, M.; Singh, V.; Hazarika, N.; Faisal, M.; Lalchandani, V.; Shukla, A.; Dave, J.; Rastogi, N.; Tripathi, S.N. Chemical speciation and source apportionment of ambient $PM_{2.5}$ in New Delhi before, during, and after the Diwali fireworks. *Atmos. Pollut. Res.* **2022**, *13*, 101428.
25. United States Geological Survey (USGS). What Minerals Produce the Colors in Fireworks? 2022. Available online: https://www.usgs.gov/media/images/what-minerals-produce-colors-fireworks (accessed on 20 May 2023).
26. Oliver, J. Fireworks Near Me: Detroit's 4th of July 2021. Available online: https://patch.com/michigan/detroit/fireworks-near-me-detroits-4th-july-2021 (accessed on 20 May 2023).
27. Michigan Live. July 4 Fireworks, Festivals and Other Events in Michigan. 2021. Available online: https://www.mlive.com/news/2021/06/july-4-fireworks-festivals-and-other-events-in-michigan.html (accessed on 20 May 2023).
28. Chou, C.L. Sulfur in coals: A review of geochemistry and origins. *Int. J. Coal Geol.* **2012**, *100*, 1–13. [CrossRef]
29. Hao, Y.; Meng, X.; Yu, X.; Lei, M.; Li, W.; Shi, F.; Xie, S. Characteristics of trace elements in $PM_{2.5}$ and PM_{10} of Chifeng, northeast China: Insights into spatiotemporal variations and sources. *Atmos. Res.* **2018**, *213*, 550–561.
30. Wang, J.; Jiang, H.; Jiang, H.; Mo, Y.; Geng, X.; Li, J.; Mao, S.; Bualert, S.; Ma, S.; Li, J.; et al. Source apportionment of water-soluble oxidative potential in ambient total suspended particulate from Bangkok: Biomass burning versus fossil fuel combustion. *Atmos. Environ.* **2020**, *235*, 117624.
31. Yu, Y.; He, S.; Wu, X.; Zhang, C.; Yao, Y.; Liao, H.; Wang, Q.; Xie, M. $PM_{2.5}$ elements at an urban site in Yangtze River Delta, China: High time-resolved measurement and the application in source apportionment. *Environ. Pollut.* **2019**, *253*, 1089–1099.
32. Farahani, V.J.; Soleimanian, E.; Pirhadi, M.; Sioutas, C. Long-term trends in concentrations and sources of $PM_{2.5}$–bound metals and elements in central Los Angeles. *Atmos. Environ.* **2021**, *253*, 118361.
33. Harrison, R.M.; Jones, A.M.; Gietl, J.; Yin, J.; Green, D.C. Estimation of the contributions of brake dust, tire wear, and resuspension to nonexhaust traffic particles derived from atmospheric measurements. *Environ. Sci. Technol.* **2012**, *46*, 6523–6529.
34. Scerri, M.M.; Genga, A.; Iacobellis, S.; Delmaire, G.; Giove, A.; Siciliano, M.; Siciliano, T.; Weinbruch, S. Investigating the plausibility of a PMF source apportionment solution derived using a small dataset: A case study from a receptor in a rural site in Apulia-South East Italy. *Chemosphere* **2019**, *236*, 124376. [PubMed]
35. Liu, W.; Xu, Y.; Liu, W.; Liu, Q.; Yu, S.; Liu, Y.; Wang, X.; Tao, S. Oxidative potential of ambient PM2. 5 in the coastal cities of the Bohai Sea, northern China: Seasonal variation and source apportionment. *Environ. Pollut.* **2018**, *236*, 514–528. [PubMed]
36. Invest Ontario. Mining. 2022. Available online: https://www.investontario.ca/mining#intro (accessed on 20 May 2023).
37. Michigan Government. Mining in Michigan: A Focus on Nonferrous Mineral Extraction. 2017. Available online: https://www.michigan.gov/-/media/Project/Websites/egle/Documents/Programs/OGMD/Mining/Guidebook.pdf?rev=3fa963fe017f40149063f83cf2f7a695#:~:text=Today%2C%20two%20iron%20mines%20remain,percent%20of%20the%20nation\T1\textquoterights%20copper (accessed on 20 May 2023).
38. The Diggings. Mining in Ohio. 2023. Available online: https://thediggings.com/usa/ohio (accessed on 20 May 2023).
39. Research Triangle Institute (RTI). Evaluation of PM2.5 Emissions and Controls at Two Michigan Steel Mills and a Coke Oven Battery. 2006. Available online: https://www.epa.gov/sites/default/files/2015-06/documents/aqm_detroit_steel_report_final_20060207.pdf (accessed on 20 May 2023).
40. Sugiyama, T.; Shimada, K.; Miura, K.; Lin, N.-H.; Kim, Y.P.; Chan, C.K.; Takami, A.; Hatakeyama, S. Measurement of ambient PAHs in Kumamoto: Differentiating local and transboundary air pollution. *Aerosol Air Qual. Res.* **2017**, *17*, 3106–3118.
41. Liu, B.; Wu, J.; Zhang, J.; Wang, L.; Yang, J.; Liang, D.; Dai, Q.; Bi, X.; Feng, Y.; Zhang, Y.; et al. Characterization and source apportionment of $PM_{2.5}$ based on error estimation from EPA PMF 5.0 model at a medium city in China. *Environ. Pollut.* **2017**, *222*, 10–22.
42. The National Aeronautics and Space Administration (NASA). A Smoky May for North America. 2023. Available online: https://earthobservatory.nasa.gov/images/151384/a-smoky-may-for-north-america (accessed on 13 July 2023).
43. Wang, S.; Hu, G.; Yan, Y.; Wang, S.; Yu, R.; Cui, J. Source apportionment of metal elements in $PM_{2.5}$ in a coastal city in Southeast China: Combined Pb-Sr-Nd isotopes with PMF method. *Atmos. Environ.* **2019**, *198*, 302–312.
44. Chi, R.; Li, H.; Wang, Q.; Zhai, Q.; Wang, D.; Wu, M.; Liu, Q.; Wu, S.; Ma, Q.; Deng, F.; et al. Association of emergency room visits for respiratory diseases with sources of ambient $PM_{2.5}$. *J. Environ. Sci.* **2019**, *86*, 154–163.
45. Ontario Environment and Energy (OEE). The End of Coal. 2021. Available online: https://www.ontario.ca/page/end-coal (accessed on 20 May 2023).

46. United States Energy Information Administration (USEIA). Michigan State Energy Profile. 2022. Available online: https://www.eia.gov/state/print.php?sid=MI#:~:text=Michigan%20Quick%20Facts&text=In%202021%2C%20coal%20provided%20the,three%2Dfifths%20of%20that%20power (accessed on 20 May 2023).
47. Sofowote, U.M.; Su, Y.; Dabek-Zlotorzynska, E.; Rastogi, A.K.; Brook, J.; Hopke, P.K. Sources and temporal variations of constrained PMF factors obtained from multiple-year receptor modeling of ambient PM2. 5 data from five speciation sites in Ontario, Canada. *Atmos. Environ.* **2015**, *108*, 140–150.
48. Choi, S.; Park, J.-H.; Kim, W.; Kim, S.W.; Lee, K.-H.; Chung, T.; Park, J.; Ryu, S.-H.; Shin, J.; Koh, D.-H.; et al. Black Carbon Exposure Characteristics in Diesel Engine Vehicle-related Jobs. *Aerosol Air Qual. Res.* **2021**, *21*, 200675.
49. Chen, R.; Zhao, Y.; Tian, Y.; Feng, X.; Feng, Y. Sources and uncertainties of health risks for $PM_{2.5}$-bound heavy metals based on synchronous online and offline filter-based measurements in a Chinese megacity. *Environ. Int.* **2022**, *164*, 107236.
50. Landis, M.S.; Lewis, C.W.; Stevens, R.K.; Keeler, G.J.; Dvonch, J.T.; Tremblay, R.T.F. McHenry tunnel study: Source profiles and mercury emissions from diesel and gasoline powered vehicles. *Atmos. Environ.* **2007**, *41*, 8711–8724.
51. Balakrishna, G.; Pervez, S.; Bisht, D.S. Source apportionment of arsenic in atmospheric dust fall out in an urban residential area, Raipur, Central India. *Atmos. Chem. Phys.* **2011**, *11*, 5141–5151.
52. Hsu, C.Y.; Chiang, H.C.; Chen, M.J.; Chuang, C.Y.; Tsen, C.M.; Fang, G.C.; Tsai, Y.I.; Chen, N.T.; Lin, T.Y.; Lin, S.L.; et al. Ambient $PM_{2.5}$ in the residential area near industrial complexes: Spatiotemporal variation, source apportionment, and health impact. *Sci. Total Environ.* **2017**, *590*, 204–214. [PubMed]
53. Taghvaee, S.; Sowlat, M.H.; Mousavi, A.; Hassanvand, M.S.; Yunesian, M.; Naddafi, K.; Sioutas, C. Source apportionment of ambient $PM_{2.5}$ in two locations in central Tehran using the Positive Matrix Factorization (PMF) model. *Sci. Total Environ.* **2018**, *628*, 672–686. [PubMed]